J. Phys. B: At. Mol. Opt. Phys. 28 (1995) 3027–3046. Printed in the UK

A scaling of multiple ionization cross sections

V Fisher, Yu Ralchenko, A Goldgirsh, D Fisher and Y Maron
Faculty of Physics, Weizmann Institute of Science, Rehovot 76100, Israel

Received 16 March 1995

Abstract. On the basis of av experimental data we demonstrate scaling laws of electron-impact multiple ionization cr ections and propose expressions for the cross sections for arbitrary atoms and ions.

1. Introduction

We consider multiple ionizations of atoms and atomic ions by electron impact:

$$\mathrm{e} + \mathrm{A}^{q+} \rightarrow \mathrm{e} + \mathrm{A}^{(q+m)+} + m\mathrm{e} \qquad m > 1. \tag{1}$$

Here, $q = 0, 1, 2, \ldots$ is the charge of a target ion (atom) A^{q+} and m is the number of electrons emitted in one collision. Cross sections of this process are studied experimentally for many atoms (mainly for $m = 2$ and 3) and for a few ions, but as yet there is no general analytical expression for the cross section applicable to an arbitrary species A^{q+} and an arbitrary number m. The incompleteness of data poses difficulties in the study of plasmas with overthermal electrons, since in these plasmas the contributions of multiple ionization events (1) to the formation of highly charged ions may dominate the contributions of consecutive single-ionization events ($m = 1$). A convincing example of the effect of multiple ionizations on the charge state distribution in plasma is presented by Müller [1].

Experimental data [2–30] demonstrate that the electron-impact multiple ionization cross sections follow two scaling laws for two ranges of the kinetic energy ϵ of the projectile electron. The first of the scaling laws is for one-step ionization, i.e. for direct ionization of the ion A^{q+} *into the ground state* of $\mathrm{A}^{(q+m)+}$. This law is valid for kinetic energy ϵ below the energy thresholds of indirect ionization and direct ionization into excited states of $\mathrm{A}^{(q+m)+}$. Experimental data demonstrating the first scaling law and our formula for multiple ionization cross section in the one-step range of energy are presented in section 2. The second law is for total (one-step plus several-step) m-fold ionization cross sections in the range of energy ϵ sufficient to involve most-contributing several-step mechanisms. This law is presented in section 3. The accuracy of scaling relations is within a factor of two for most of the experimentally studied multiple ionization cross sections. On the basis of the scaling laws, in section 4 we propose expressions for estimating m-fold ionization cross sections $\sigma_{\mathrm{A},q,m}(\epsilon)$ for arbitrary species A^{q+} and energy ϵ. Applicability of the scaling laws to multiple ionization of negative ions A^- is discussed in section 5.

2. First scaling law

Let $I_{A,q,m}$ be the minimal energy required for the extraction of m electrons from the ground state of A^{q+} by a single electron impact, and let $I'_{A,q,m}$ be the sum of ionization potentials $I_{A,k}$ of species from A^{q+} to $A^{(q+m^{-1})+}$, i.e.

$$I'_{A,q,m} = \sum_{k=q}^{q+m-1} I_{A,k}.$$

To our knowledge no data are available for $I_{A,q,m}$, except for the values which may be inferred from the experimentally determined cross sections [2–30]. The accuracy of these values is generally better than 20% and within this accuracy

$$I_{A,q,m} \approx I'_{A,q,m} \tag{2}$$

Let us introduce the scaled kinetic energy of a projectile electron

$$x = \frac{\epsilon}{I_{A,q,m}}$$

and scaled cross section

$$\tilde{\sigma}^{d}_{A,q,m}(x) = \frac{\sigma^{\exp}_{A,q,m}(x)}{S^{d}_{A,q,m}}. \tag{3}$$

Here $\sigma^{\exp}_{A,q,m}(\epsilon)$ is the experimentally determined cross section, the quantity

$$S^{d}_{A,q,m} = \frac{\pi a_0^2}{17^{m-1}} \left(\frac{I_H}{I_{A,q,m}}\right)^2 \zeta^{d}_{A,q,m} \tag{4}$$

is the scaling factor, a_0 is the Bohr radius, I_H is the ionization potential of the hydrogen atom and $\zeta^{d}_{A,q,m}$ is the number of ways for one-step ionization, i.e. for direct m-fold ionization into the ground state of $A^{(q+m)+}$. This number is calculated as follows. Let ξ_o and ξ_s be the numbers of electrons in the outermost and sub-outermost n shells of A^{q+}. If $\xi_o > m$, then one-step ionization is due to direct removal of m electrons from the outermost shell and $\zeta^{d}_{A,q,m}$ is the number of ways to select m electrons from ξ_o:

$$\zeta^{d}_{A,q,m} = \frac{\xi_o!}{m!(\xi_o - m)!} \qquad \xi_o \geqslant m. \tag{5}$$

If $\xi_o < m$, the one-step m-fold ionization removes ξ_o electrons of the outermost shell, and $m' = (m - \xi_o)$ electrons from the sub-outermost n shell. In this case the coefficient $\zeta^{d}_{A,q,m}$ is the number of ways to select m' electrons from ξ_s:

$$\zeta^{d}_{A,q,m} = \frac{\xi_s!}{m'!(\xi_s - m')!} \qquad \xi_o < m. \tag{6}$$

We found that for each experimentally determined cross section $\sigma^{\exp}_{A,q,m}(\epsilon)$ there is an energy range $1 \leqslant x \leqslant x^{i}_{A,q,m}$ for which the scaled cross section (3) equals approximately the scaled cross sections $\tilde{\sigma}^{\mathrm{d}}_{\mathrm{A},q,m}(x)$ of all other species (in their ranges $x \leqslant x^{\mathrm{i}}_{\mathrm{A},q,m}$). This observation may be presented by a scaling law

$$\tilde{\sigma}^{\mathrm{d}}_{\mathrm{A},q,m}(x) \approx \tilde{\sigma}^{\mathrm{d}}_{\mathrm{u}}(x) \qquad 1 \leqslant x \leqslant x^{\mathrm{i}}_{\mathrm{A},q,m} \tag{7}$$

with $\tilde{\sigma}^{\mathrm{d}}_{\mathrm{u}}(x)$ being the universal (independent on A, q, and m) cross section. Behaviour of the cross sections $\sigma^{\mathrm{exp}}_{\mathrm{A},q,m}(x)$ for $x > x^{\mathrm{i}}_{\mathrm{A},q,m}$ shows that the validity limit $x^{\mathrm{i}}_{\mathrm{A},q,m}$ is the minimal energy required for several-step multiple ionization mechanisms, such as inner-shell ionization followed by autoionization, inner-shell excitation followed by autoionization, resonant-excitation–triple-autoionization, other indirect mechanisms [31–33], or direct m-fold ionization into excited state of $\mathrm{A}^{(q+m)+}$ followed by radiative transitions into its ground state.

In figure 1, we present cross sections $\tilde{\sigma}^{\mathrm{d}}_{\mathrm{A},q,m}(x)$ of species which have the largest values of $x^{\mathrm{i}}_{\mathrm{A},q,m}$. The figure illustrates the scaling relation (7) and demonstrates the shape of the cross section $\tilde{\sigma}^{\mathrm{d}}_{\mathrm{u}}(x)$. This shape may be fitted well by the function

$$\tilde{\sigma}^{\mathrm{d}}_{\mathrm{u}}(x) = 4\frac{\ln x}{x^{1.4}}\left(1 - 2\mathrm{e}^{-0.7x}\right) \qquad 1 \leqslant x \leqslant x^{\mathrm{i}}_{\mathrm{A},q,m} \tag{8}$$

shown by the thick full curve. For certain species, cross sections were measured by a few research groups, but for clarity in the figure, we present in figure 1(a) only one set of experimental data for each cross section (usually the most recent results, or the results obtained in a larger energy range). To illustrate the spread in the experimental data, we present in figure 1(b) seven experimental curves $\tilde{\sigma}^{\mathrm{d}}_{\mathrm{A},q,m}(x)$ obtained for three cross sections. One can see that at any energy x, the spread in the experimental data for each cross section and the deviation of these data from the scaling law (7) are about the same.

The scaling of the cross sections demonstrated in figure 1 is an argument for expecting the same scaling for all values of A, q and m. Then the general expression for electron-impact multiple ionization cross section in the one-step ionization range may be presented as

$$\sigma_{\mathrm{A},q,m}(x) = S^{\mathrm{d}}_{\mathrm{A},q,m}\tilde{\sigma}^{\mathrm{d}}_{\mathrm{u}}(x) \qquad 1 \leqslant x \leqslant x^{\mathrm{i}}_{\mathrm{A},q,m}. \tag{9}$$

Taking into account (4) and (8) this expression may be written as

$$\sigma_{\mathrm{A},q,m}(x) = \frac{4\pi a_0^2}{17^{m-1}}\left(\frac{I_{\mathrm{H}}}{I_{\mathrm{A},q,m}}\right)^2 \zeta^{\mathrm{d}}_{\mathrm{A},q,m}\frac{\ln x}{x^{1.4}}\left(1 - 2\mathrm{e}^{-0.7x}\right) \qquad x \leqslant x^{\mathrm{i}}_{\mathrm{A},q,m}. \tag{10}$$

Up to now, to analyse the dependence of validity limits $x^{\mathrm{i}}_{\mathrm{A},q,m}$ on q and m, data are available for argon only. One can see in table 1 that $x^{\mathrm{i}}_{\mathrm{A},q,m}$ decreases with increasing q at a given m, and with increasing m at a given q.

For electron energy in the near-threshold range Wannier [34] predicted power dependence of the cross sections on $(\epsilon - I_{\mathrm{A},q,m})$:

$$\sigma_{\mathrm{A},q,m} \sim (x - 1)^{w} \tag{11}$$

with the exponent w equal to or slightly larger than the number of removed electrons. It may be presented as $w = m + \delta$ with $\delta \ll 1$. Our formula (10) results in the exponent $w = 2$ (to be rigorous here, the coefficient 0.7 in (10) has to be replaced by $\ln 2 \approx 0.6931$).

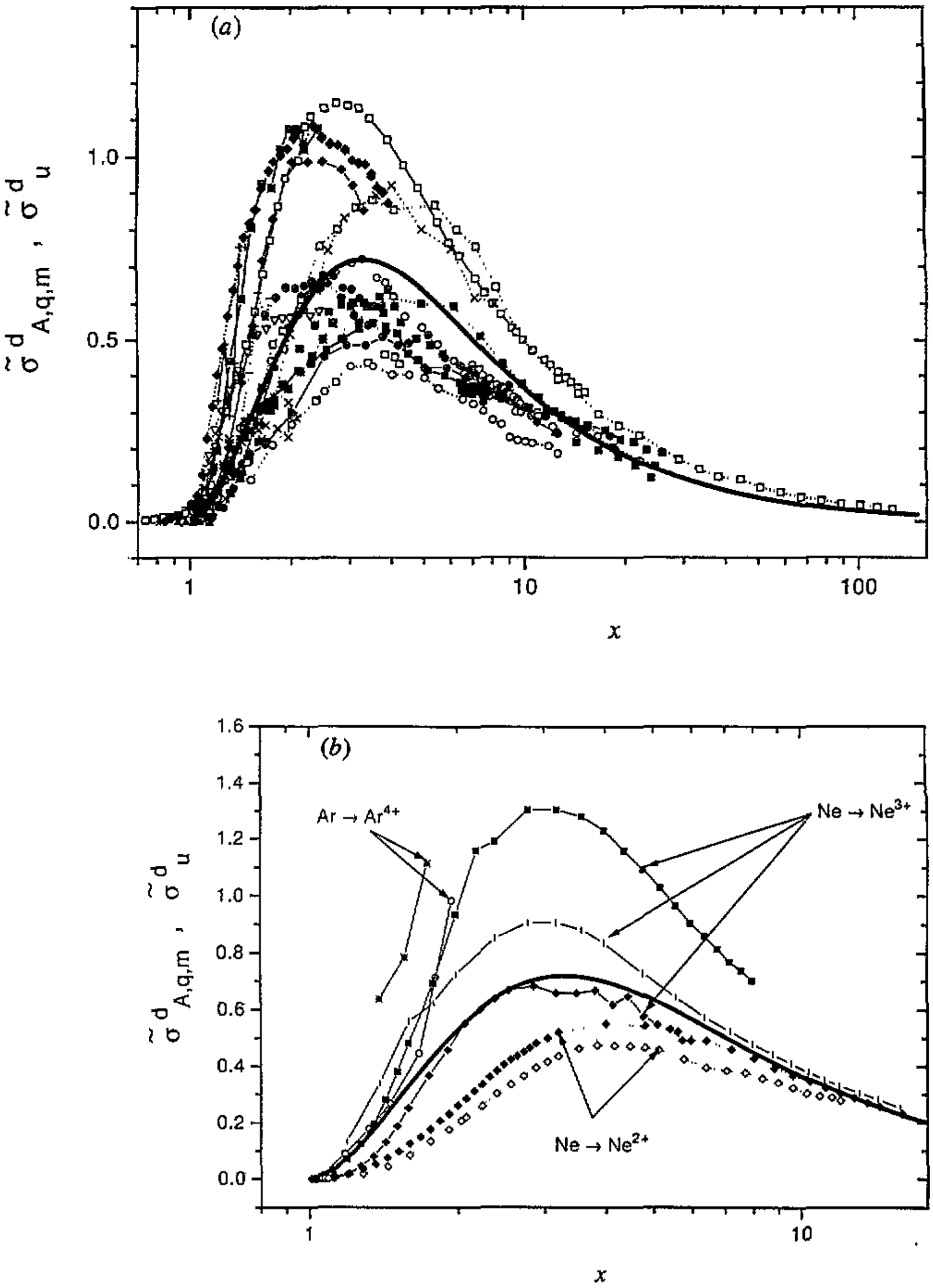

Figure 1. Universal cross section (8)—thick full curve, compared with scaled double, triple and fourfold ionization cross sections $\tilde{\sigma}^{\rm d}_{{\rm A},q,m}(x)$ of various atoms and ions in the one-step ionization range $x \leqslant x^{\rm i}_{{\rm A},q,m}$. Notations and references are listed in table 1.

Table 1. Notations and references to figure 1. The missing value of $x^{\mathrm{i}}_{\mathrm{A},q,m}$ corresponds to one-step multiple ionization in the entire studied range of the energy of the projectile electron or to the relatively small (indistinguishable) contribution of several-step processes. Letters a and b in the first column point to the figures 1(a) or 1(b) where the symbol is used.

Symbol in figure 1		A^{q+}	Atomic number	m	w	$x^{\mathrm{i}}_{\mathrm{A},q,m}$	Studied range of energy x	Reference
- -□- -	a	He	2	2	1.7		1.1–127	Shah *et al* [23]
- -■- -	a	Li	3	2			3.5–25	Jalin *et al* [11]
- -○- -	a	Li^+	3	2	1.5		1.5–12.5	Peart and Dolder [21]
□	a	C^+	6	2	0.4	4.3	0.9–35	Zambra *et al* [29]
■	a	N^+	7	2	0.5		0.9–26	Zambra *et al* [29]
- -x- -	a	O	8	2	2.3		0.9–8	Ziegler *et al* [30]
○	a	O^+	8	2	2		0.9–22	Zambra *et al* [29]
- -◇- -	b	Ne	10	2	2		1–12	Lebius *et al* [13]
- -◆- -	b	Ne	10	2	1.6		1.1–16	Krishnakumar and
–■–	b	Ne	10	3	1.5		1–8	Srivastava [12]
–◆–	b	Ne	10	3	2.5		1–6	Lebius *et al* [13]
–|–	b	Ne	10	3	1.3		1.1–16	Gaudin [9]
–●–	a	Ne	10	4	4.1		1–3.3	Lebius *et al* [13]
●	a	Ne^+	10	2	1.9		1–24	Zambra *et al* [29]
–⊕–	a	Na^+	11	2	0.13		1–12.5	Hirayama [10]
–⊗–	a	Mg	12	2	1.8	2.42	1–233	McCallion *et al* [14]
–□–	a	Ar	18	2	0.42		0.7–15	Syage [25]
–◆–	a	Ar	18	3	1.9	3.33	1.1–7.9	Syage [25]
–○–	b	Ar	18	4	1.27	1.95	1.1–4.6	Syage [25]
–*–	b	Ar	18	4	0.85	1.74	1.4–14	Gaudin [9]
- -◆- -	a	Ar^+	18	2	2.3	3.95	0.8–9.5	Müller *et al* [17]
–x–	a	Ar^+	18	3	1.5	2.08	1.1–6.5	Müller and Frodl [16]
- -∇- -	a	Ar^{2+}	18	2	1.6	2.44	0.95–10	Tinschert *et al* [26]
–+–	a	Ar^{2+}	18	3	1.5	1.47	1.2–4.7	Müller and Frodl [16]
- -*- -	a	Ar^{3+}	18	2	0.7	1.78	0.8–7.5	Tinschert *et al* [26]
- -—- -	a	Ar^{4+}	18	2	2.8	1.73	0.96–10	Müller *et al* [17]
- -⊕- -	a	K^+	19	2	1.5		1.1–18	Hirayama *et al* [10]
- -⊗- -	a	Cu	29	2	1.9	4.1	1.2–70	Bolorizadeh *et al* [2]

One can see in table 1 that in the case of double ionization ($m = 2$) twelve experimental curves from the eighteen available ones give w in the range 2 ± 0.5, i.e. both $w = 2$ and $w = m + \delta$ fit two-thirds of the measurements within a deviation of ± 0.5. In the cases of threefold and fourfold ionization (a total of nine experimental curves) five curves show $w = 2$ while $w \approx m$ is shown by only two curves (within the same deviation of ± 0.5). To make a final conclusion on the behaviour of the cross sections at $x \approx 1$, more experimental data of high accuracy are required.

The only analytical expression related to multiple ionization is that given by Gryzinski [35] for direct double ionization cross sections:

$$\tilde{\sigma}^{\mathrm{Gryz}}_{\mathrm{A},q,2}(x) = \frac{\xi_0(\xi_0 - 1)}{4\pi\bar{r}^2}\frac{\sigma_0}{I_q^2}\frac{\sigma_0}{I_{q+1}^2}g(x). \tag{12}$$

Here, $\sigma_0 = 4\pi a_0^2 I_{\mathrm{H}}^2$, $\bar{r}$ is the mean distance between electrons in the outer shell and $g(x)$ is the function given by Gryzinski in graphical form for $x \leqslant 32$. Müller [31] approximated this function as

$$g(x) = \frac{\ln x}{1.59x^2 - 3.71x + 16.2} + 2.14 \times 10^{-4}(x - 1) - 3.67 \times 10^{-6}(x - 1)^2.$$

In deriving expression (12), Gryzinski treated the direct double ionization as the consecutive removal of two electrons from the outer n-shell. Electrons of the outer shell were assumed to be distributed homogeneously over a sphere of radius R equal to the mean radius of the target particle A^{q+}. The distance $\bar{r}$ was expressed by

$$\bar{r} = R\xi_0^{-1/3}. \tag{13}$$

As long as the mean radius of the atomic particles is not a strictly defined term, we can express R in the terms of mean distance $\langle r\rangle$ of the outer electrons from the nucleus:

$$R = \gamma\langle r\rangle \tag{14}$$

where γ is a coefficient expected to be nearly independent of the species. The distance $\langle r\rangle$ is defined as

$$\langle r\rangle = \int_0^\infty r|\psi^2|\mathrm{d}r \tag{15}$$

with $\psi(\boldsymbol{r})$ being the wavefunction of electrons in the outer shell.

For atoms, $\langle r\rangle$ is known from Radzig and Smirnov [36]. For the ions listed in table 1, we calculated $\psi(\boldsymbol{r})$ and $\langle r\rangle$ in the Hartree–Fock with relativistic corrections approximation [37]. To estimate γ we express $\bar{r}$ using the formulae (13) and (14): $\bar{r} = \gamma\langle r\rangle\xi_0^{-1/3}$, and calculate 14 functions $\gamma(x)$ for 14 species using the equations

$$\sigma^{\mathrm{Gryz}}_{\mathrm{A},q,2}(x) = \sigma^{\mathrm{exp}}_{\mathrm{A},q,2,}(x) \qquad x < x^{\mathrm{i}}_{\mathrm{A},q,m}. \tag{16}$$

The cross sections $\sigma^{\mathrm{exp}}_{\mathrm{A},q,2}(x)$ are taken from the references listed in table 1. The functions $\gamma(x)$ are presented in figure 2. In the range $x > 2$ the deviation of these functions from the average value $\bar{\gamma} = 2.1$ is within a factor $f_{\mathrm{G}} = 1.8$. Based on figure 2, one may expect that direct double ionization cross sections, calculated using the formula by Gryzinski (12) with $\bar{r} = \gamma\langle r\rangle/\xi_0^{1/3}$ and $\gamma = 2.1$, will be accurate within a factor of $f_{\mathrm{G}}^2 = 3.2$ in the energy range $x > 2$. Note that our formula (10) provides an accuracy within a factor of two in this range and is applicable for arbitrary m.

3. Second scaling law

Analysis of the experimentally determined multiple ionization cross sections [2–30] in the energy range $x > x^{\mathrm{i}}_{\mathrm{A},q,m}$ shows the second scaling law for species which have twelve or more electrons. This law is valid for projectile electron energy above the threshold value $x^{\mathrm{t}}_{\mathrm{A},q,m}$, which is the minimal energy required for *most* of the several-step mechanisms of multiple ionization. By the definitions of $x^{\mathrm{i}}_{\mathrm{A},q,m}$ and $x^{\mathrm{t}}_{\mathrm{A},q,m}$, $x^{\mathrm{t}}_{\mathrm{A},q,m}$ is always larger than $x^{\mathrm{i}}_{\mathrm{A},q,m}$.

To demonstrate the scaling of experimentally determined multiple ionization cross sections [2–30] in the energy range $x > x^{\mathrm{t}}_{\mathrm{A},q,m}$ it is convenient to introduce scaling factors $S^{\mathrm{t}}_{\mathrm{A},q,m}$ by the expression

$$S^{\mathrm{t}}_{\mathrm{A},q,m}(x) = \frac{\pi a_0^2}{17^{m-1}}\left(\frac{I_{\mathrm{H}}}{I_{\mathrm{A},q,m}}\right)^2 \zeta^{\mathrm{t}}_{\mathrm{A},q,m} \tag{17}$$

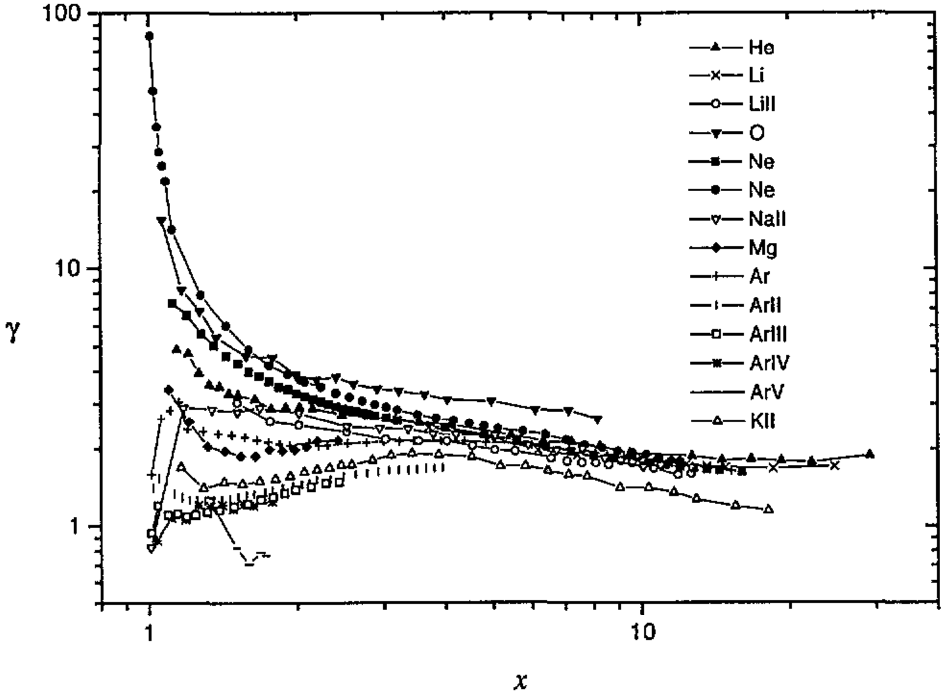

Figure 2. The function $\gamma(x)$ calculated from the best fit of the formula by Gryzinski (12) to experimentally determined cross sections $\sigma^{\mathrm{exp}}_{\mathrm{A},q,2}(\epsilon)$ of fourteen species from table 1.

and scaled cross sections $\tilde{\sigma}^{\mathrm{t}}_{\mathrm{A},q,m}(x)$ by the expression

$$\tilde{\sigma}^{\mathrm{t}}_{\mathrm{A},q,m}(x) = \frac{\sigma^{\mathrm{exp}}_{\mathrm{A},q,m}(x)}{S^{\mathrm{t}}_{\mathrm{A},q,m}} \qquad x > x^{\mathrm{t}}_{\mathrm{A},q,m}. \tag{18}$$

The coefficient $\zeta^{\mathrm{t}}_{\mathrm{A},q,m}$ is the total number of ways to remove m electrons by one electron impact:

$$\zeta^{\mathrm{t}}_{\mathrm{A},q,m} = \zeta^{\mathrm{d}}_{\mathrm{A},q,m} + \zeta^{\mathrm{f}}_{\mathrm{A},q,m}. \tag{19}$$

The number of ways provided by a one-step mechanism, $\zeta^{\mathrm{d}}_{\mathrm{A},q,m}$, is given by formulae (5) and (6). The term $\zeta^{\mathrm{f}}_{\mathrm{A},q,m}$ is the number of ways provided by all several-step mechanisms. Analysing experimentally determined cross sections [2–30], we found that the scaling of $\sigma^{\mathrm{t}}_{\mathrm{A},q,m}(x)$ is obtained when $\zeta^{\mathrm{f}}_{\mathrm{A},q,m}$ is taken as

$$\zeta^{\mathrm{f}}_{\mathrm{A},q,m} = \frac{\xi^{\mathrm{f}}_{\mathrm{A},q,m}!}{m!(\xi^{\mathrm{f}}_{\mathrm{A},q,m} - m)!} \tag{20}$$

with $\xi^{\mathrm{f}}_{\mathrm{A},q,m}$ being the total number of electrons in the subshells participating in the m-fold ionization. This number is determined by the expressions (24)–(27) below.

The fact that to obtain the scaling of experimentally determined cross sections, we had to take the number of ways $\zeta^{\mathrm{f}}_{\mathrm{A},q,m}$ equal to binomial coefficient (20), is experimental evidence of a weakness of correlations between electrons for most of the atoms (ions) studied. Being interested in a single simple formula for all A, q, m, we are always using the approximation of uncorrelated electrons though it may be rather rough for some species.

In figure 3, we present scaled experimental cross sections $\tilde{\sigma}^{\mathrm{t}}_{\mathrm{A},q,m}(x)$ of species which have 12 or more electrons (notations and references for this figure are given in table 2). For clarity in the figures, 88 curves $\tilde{\sigma}^{\mathrm{t}}_{\mathrm{A},q,m}(x)$ are divided into four groups according to atomic numbers of target atoms or ions and presented in four graphs. The cross sections are presented in th range $x \geqslant x^{\mathrm{t}}_{\mathrm{A},q,m}$ where they depend on A, q, and m rather weakly, i.e. demonstrate the scaling law

$$\tilde{\sigma}^{\mathrm{t}}_{\mathrm{A},q,m}(x) \approx \tilde{\sigma}^{\mathrm{t}}_{\mathrm{u}}(x) \qquad x > x^{\mathrm{t}}_{\mathrm{A},q,m}. \tag{21}$$

Function $\sigma^{\mathrm{t}}_{\mathrm{u}}(x)$ may be fitted well by the expression

$$\tilde{\sigma}^{\mathrm{t}}_{\mathrm{u}}(x) = 1.6\frac{\ln x}{x^{0.9}}\left(1 - 2\mathrm{e}^{-0.7x}\right) \qquad x > x^{\mathrm{t}}_{\mathrm{A},q,m} \tag{22}$$

which is shown in figure 3 by the thick full curve. Thresholds $x^{\mathrm{t}}_{\mathrm{A},q,m}$ inferred from the experimental data are given in table 2. The accuracy of these values is about 10%. The inequality sign before a value means that for this atom the scaling relation (21) is correct in the entire range of energy studied experimentally, i.e. $x^{\mathrm{t}}_{\mathrm{A},q,m}$ is smaller than the minimal experimentally studied energy (given in the table).

The accuracy of the scaling laws (7) and (21) may be illustrated by a distribution of deviations of experimental data from universal cross sections $\tilde{\sigma}^{\mathrm{t}}_{\mathrm{u}}(x)$ and $\tilde{\sigma}^{\mathrm{d}}_{\mathrm{u}}(x)$. Let us introduce the deviations D^{t} and D^{d} by expressions

$$D^{\mathrm{t}}_{\mathrm{A},q,m}(x) = \frac{|\tilde{\sigma}^{\mathrm{t}}_{\mathrm{A},q,m}(x) - \tilde{\sigma}^{\mathrm{t}}_{\mathrm{u}}(x)|}{\tilde{\sigma}^{\mathrm{t}}_{\mathrm{u}}(x)} \qquad D^{\mathrm{d}}_{\mathrm{A},q,m}(x) = \frac{|\tilde{\sigma}^{d}_{\mathrm{A},q,m} - \tilde{\sigma}^{\mathrm{d}}_{\mathrm{u}}(x)|}{\tilde{\sigma}^{\mathrm{d}}_{\mathrm{u}}(x)}. \tag{23}$$

The distribution of these deviations for all experimental points shown in figures 1 and 3 (total 2684 points) is presented by the histogram in figure 4. It is seen that 90% of the points diverge from the corresponding $\tilde{\sigma}_{\mathrm{u}}(x)$ by less than a factor of two.

A search for the best fit of formula (21) to experimental data lead us to simple rules for determining the number $\xi^{\mathrm{f}}_{\mathrm{A},q,m}$ in formula (20). For a more concise explanation of these rules we introduce a few definitions and notations. Let $n_1, n_2, n_3, n_4, \ldots$ be the principal quantum numbers of electron shells of target particle A^{q+} in the ground state ($n_1 > n_2 > n_3 > n_4 \ldots$). Usually the n_1 shell is called the outermost shell, but here we make one exception to this definition, namely, if the n_1 shell contains only one or two electrons and the n_2 shell contains an empty d subshell, we consider all electrons of n_1 and n_2 shells together as one outermost shell. For example, $3\mathrm{s}^2 3\mathrm{p}^6 4\mathrm{s}^2$ electrons of Ca, $5\mathrm{s}^2 5\mathrm{p}^6 6\mathrm{s}^2$ electrons of Ba and La^+, or $5\mathrm{s}^2 5\mathrm{p}^6 6\mathrm{s}$ electrons of Ba^+ and La^{2+} are counted as the outermost shells containing 10 and 9 electrons respectively. We suppose that $5\mathrm{s}^2 5\mathrm{p}^6 5\mathrm{d}6\mathrm{s}^2$ electrons of La and Gd also have to be considered as the outermost shell, because 5d electrons in these elements actually do not open the 5d subshell: elements which follow La and Gd in the periodic table (Ce, Pr, Nd, … and Tb, Dy, Ho, …) have no 5d electrons.

The outermost shell is denoted here by O. The electron shell below the outermost one is called the sub-outermost n-shell, or S shell. The numbers of electrons in the O shell and S shell are denoted by ξ_{o} and ξ_{s} respectively. Let l_1 be the maximal orbital quantum number of S-shell electrons of A^{q+} in the ground state. The l_1 subshell of the S shell is called the S_1 subshell, with its number of electrons denoted by $\xi_{\mathrm{s}1}$.

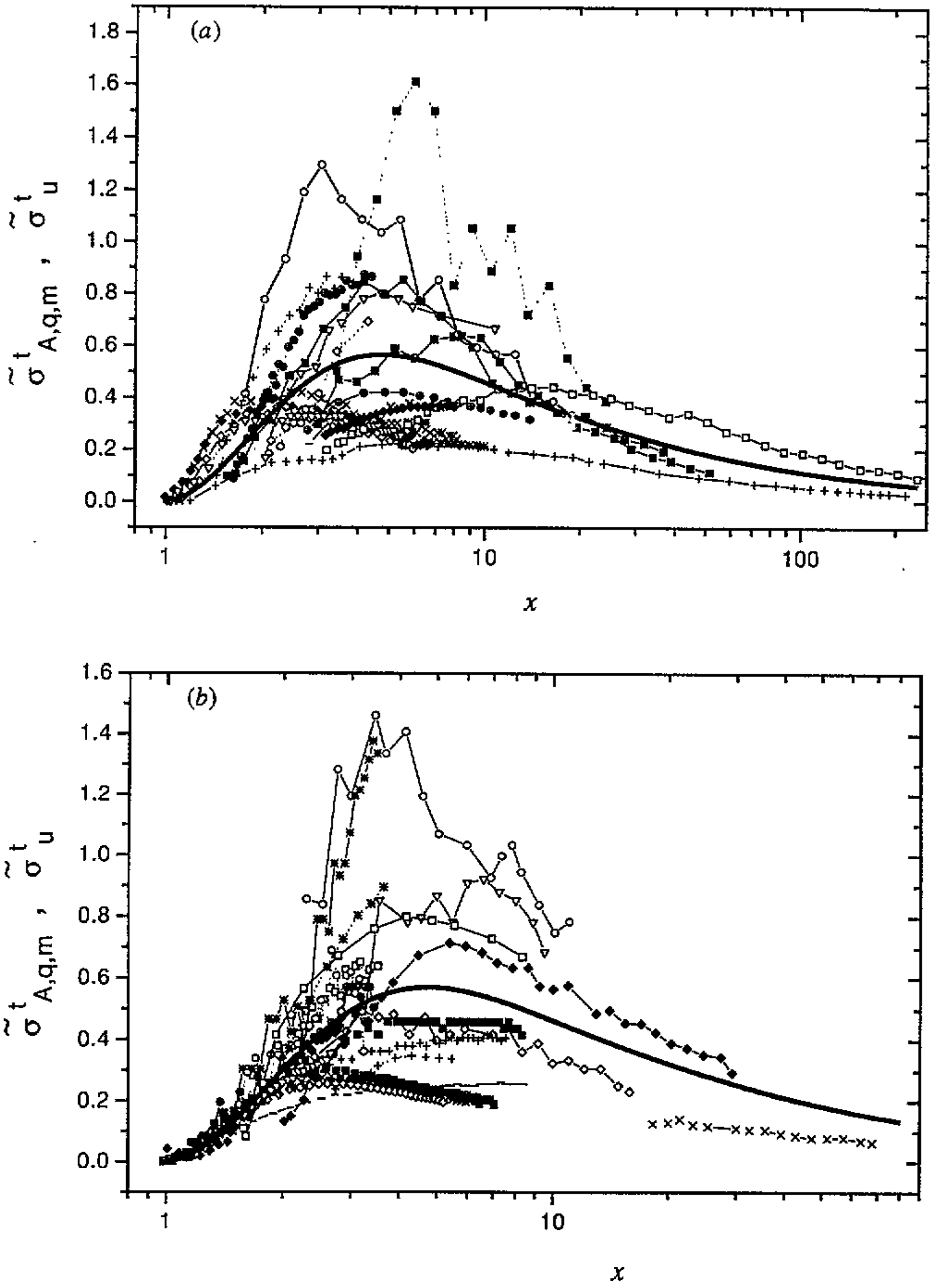

Figure 3. Universal cross section (22)—thick full curve, compared with scaled multiple ionization cross sections, $\tilde{\sigma}^t_{A,q,m}(x)$ of various atoms and ions in the energy range $x > x^t_{A,q,m}$. Notations and references are listed in table 2. For clarity in the figure, experimental data are divided in four graphs according to atomic numbers, namely (a) Mg–Ar, (b) Ca–Kr, (c) Rb–Bi excluding lanthanoids, and (d) lanthanoids.

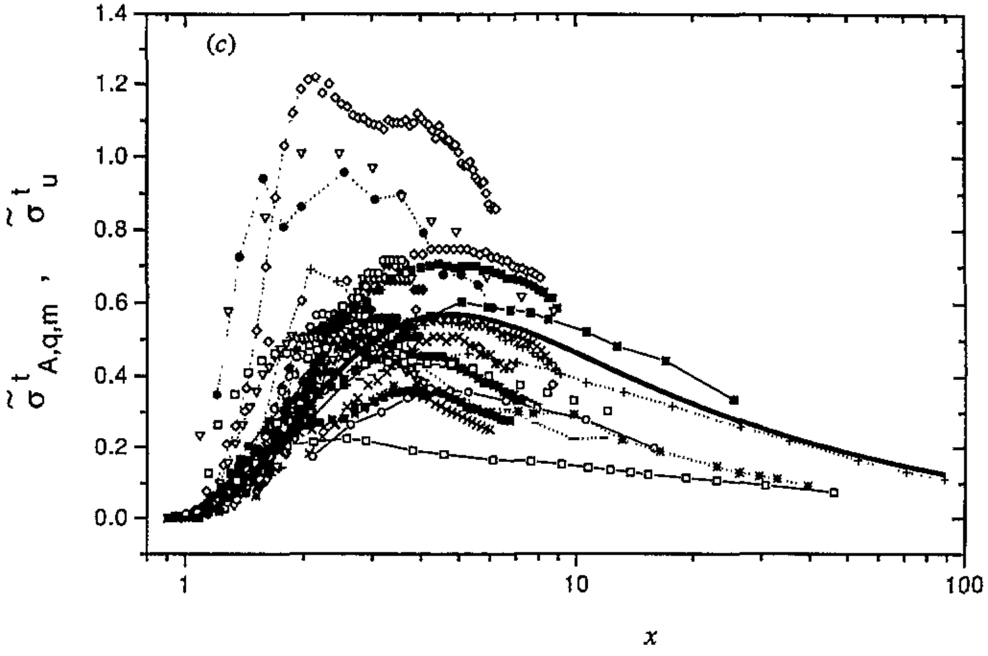

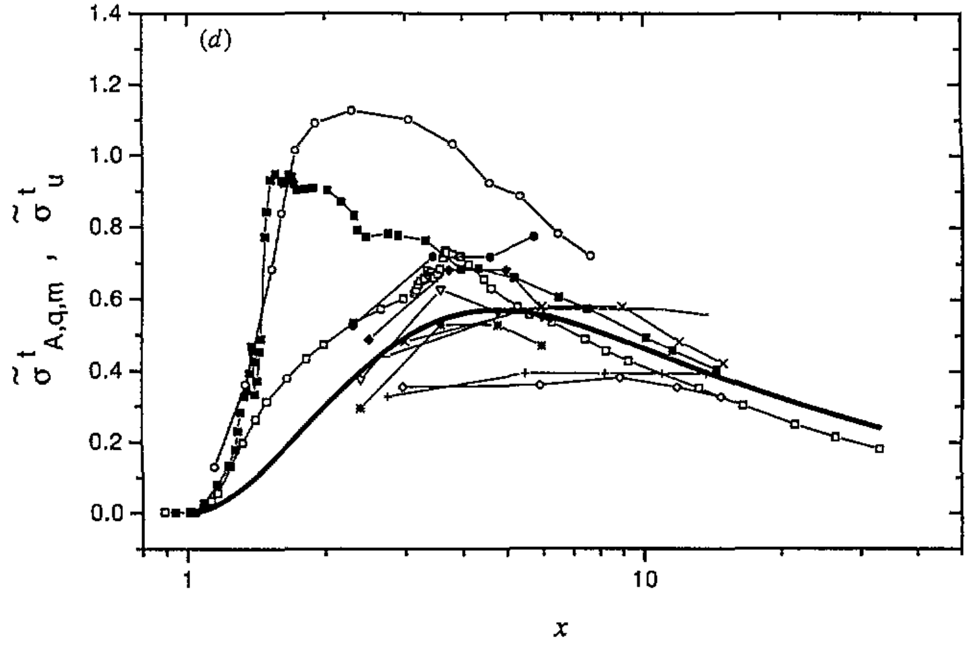

Figure 3. (Continued)

To obtain the scaling (21) a number of electrons $\xi^{\mathrm{f}}_{\mathrm{A},q,m}$ in formula (20) has to be taken according to the rules as follows:

(i) For double ionization

$$\xi^{\mathrm{f}}_{\mathrm{A},q,2} = \xi_{\mathrm{o}} + \xi_{\mathrm{s1}}. \tag{24}$$

Table 2. Notations and references to figure 3. Letters *a*, *b*, *c*, *d* in the first column point to the figures 3(a), 3(b), 3(c) or 3(d) where the symbol is used.

Symbol in figure 3		A^{q+}	Atomic number	m		$x^{t}_{A,q,m}$	Reference
-□-	a	Mg	12	2		5.7	McCallion *et al* [14]
-■-	a	Mg	12	3	<	1.5	McCallion *et al* [14]
-○-	a	Mg	12	4	<	1.7	McCallion *et al* [14]
-×-	a	Si	14	2	<	1.1	Freund *et al* [5]
-♦-	a	P	15	2		1.0	Freund *et al* [5]
-◊-	a	S	16	2		1.0	Freund *et al* [5]
- -×- -	a	S	16	3	<	4.3	Ziegler *et al* [30]
- -◊- -	a	S	16	4	<	1.3	Ziegler *et al* [30]
- -▽- -	a	Cl	17	2		1.0	Freund *et al* [5]
-+-	a	Ar	18	3		3.6	Nagy *et al* [20]
-⊕-	a	Ar	18	4		1.6	Gaudin *et al* [9]
-⊗-	a	Ar	18	4		3.0	McCallion *et al* [15]
- -□- -	a	Ar	18	4		3.2	Syage [25]
- -■- -	a	Ar	18	5	<	3.4	McCallion *et al* [15]
- -○- -	a	Ar	18	5		2.1	Syage [25]
-*-	a	Ar^{+}	18	3		5.2	Müller and Frodl [16]
- -*- -	a	Ar^{2+}	18	2		6.3	Tinschert *et al* [26]
---	a	Ar^{2+}	18	3		2.8	Müller and Frodl [16]
- -♦- -	a	Ar^{3+}	18	2		3.1	Tinschert *et al* [26]
-▽-	a	Ar^{4+}	18	2		2.0	Müller *et al* [17]
- -⊕- -	a	Ar^{5+}	18	2		1.6	Tinschert *et al* [26]
- -+- -	a	Ar^{6+}	18	2	<	1.4	Tinschert *et al* [26]
-□-	b	Ca	20	2		1.6	Chatterjee and Roy [3]
-■-	b	Fe	26	2		1.0	Freund *et al* [5]
-○-	b	Fe	26	4	<	2.3	Shah *et al* [23]
-×-	b	Cu	29	2		24.7	Bolorizadeh *et al* [2]
-♦-	b	Cu	29	3		3.62	Bolorizadeh *et al* [2]
-◊-	b	Cu	29	4		2.2	Bolorizadeh *et al* [2]
-▽-	b	Cu	29	5		1.5	Bolorizadeh *et al* [2]
-+-	b	Ga	31	2		1.0	Freund *et al* [5]
-*-	b	Ga	21	3	<	1.4	Freund *et al* [5]
---	b	Ge	32	2		1.0	Freund *et al* [5]
-⊕-	b	Ge	32	3	<	1.3	Freund *et al* [5]
-⊗-	b	As	33	2		1.0	Freund *et al* [5]
- -□- -	b	As	33	3	<	1.2	Freund *et al* [5]
- -■- -	b	Se	34	2		1.0	Freund *et al* [5]
- -○- -	b	Se	34	3	<	1.5	Freund *et al* [5]
- -×- -	b	Br	35	2	<	1.2	Hayes *et al* [6]
- -♦- -	b	Br	35	3		1.1	Hayes *et al* [6]
- -◊- -	b	Kr	36	2	<	1.2	Wetzel *et al* [28]
- -▽- -	b	Kr	36	3	<	1.2	Wetzel *et al* [28]
- -+- -	b	Kr	36	4	<	2.7	Lebius *et al* [13]
- -*- -	b	Kr	36	5	<	1.8	Lebius *et al* [13]
figure 6		Kr	36	6		1.5	Lebius *et al* [13]
figure 6		Kr	36	7		1.6	Lebius *et al* [13]
figure 6		Kr	36	8		1.5	Lebius *et al* [13]
-□-	c	Rb^{+}	37	2		1.0	Hughes and Feeney [8]
-■-	c	Rb^{+}	37	3	<	1.2	Hughes and Feeney [8]
-○-	c	Rb^{+}	37	4		2.1	Hughes and Feeney [8]
-×-	c	Ag	47	2		2.0	Freund *et al* [5]
-♦-	c	Ag	47	3		1.6	Freund *et al* [5]
-◊-	c	In	49	2		1.0	Freund *et al* [5]
-▽-	c	In	49	3		1.3	Freund *et al* [5]

Table 2. (continued)

Symbol in figure 3		A^{q+}	Atomic number	m	$x^{\mathrm{i}}_{\mathrm{A},q,m}$	Reference
-+-	c	Sn	50	2	1.0	Freund *et al* [5]
-*-	c	Sn	50	3	< 1.5	Freund *et al* [5]
- — -	c	Sb	51	2	1.0	Freund *et al* [5]
-⊕-	c	Sb	51	3	< 1.5	Freund *et al* [5]
-⊗-	c	Te	52	2	1.0	Freund *et al* [5]
- -□- -	c	Te	52	3	1.1	Freund *et al* [5]
- -■- -	c	I	53	2	1.0	Hayes *et al* [6]
- -○- -	c	I	53	3	< 1.3	Hayes *et al* [6]
- -×- -	c	Xe	54	2	1.0	Wetzel *et al* [28]
- -◆- -	c	Xe	54	3	< 1.1	Wetzel *et al* [28]
- -◇- -	c	Xe	54	4	< 1.1	Krishnakumar and Srivastava [12]
- -▽- -	c	Xe	54	5	< 1.1	
- -+- -	c	Cs^+	55	2	< 1.2	Hertling *et al* [7]
- -*- -	c	Ba	56	2	< 1.5	Dettman and Karstensen [4]
- - — - -	c	Ba	56	3	< 1.2	Dettman and Karstensen [4]
- -⊕- -	c	Ba	56	4	< 1.2	Dettman and Karstensen [4]
- -⊗- -	c	Ba^+	56	2	< 1.1	Peart *et al* [22]
□	c	Ba^{2+}	56	2	< 1.1	Tinschert *et al* [28]
-□-	d	La^+	57	2	1.0	Müller *et al* [19]
-■-	d	La^{2+}	57	2	1.0	Müller *et al* [19]
-○-	d	La^{2+}	57	3	< 1.2	Müller *et al* [19]
-×-	d	Sm	62	2	< 3.0	Shimon *et al* [24]
-◆-	d	Sm	62	3	< 2.5	Shimon *et al* [24]
-◇-	d	Eu	63	2	< 3.0	Shimon *et al* [24]
-▽-	d	Eu	63	3	< 2.4	Shimon *et al* [24]
-+-	d	Tm	69	2	< 2.7	Shimon *et al* [24]
-*-	d	Tm	69	3	< 2.4	Shimon *et al* [24]
— — —	d	Yb	70	2	< 2.7	Shimon *et al* [24]
-⊕-	d	Yb	70	3	< 2.3	Shimon *et al* [24]
■	c	Pb	82	2	1.0	Freund *et al* [5]
○	c	Pb	82	2	< 1.4	Freund *et al* [5]
×	c	Bi	83	2	1.0	Freund *et al* [5]
◆	c	Bi	83	3	< 1.3	Freund *et al* [5]
◇	c	Bi^{2+}	83	2	1.0	Müller *et al* [18]
▽	c	Bi^{3+}	83	2	1.0	Müller *et al* [18]

(ii) For fourfold ionization

$$\xi^{\mathrm{f}}_{\mathrm{A},q,4} = \xi_{\mathrm{o}} + \xi_{\mathrm{s}}. \tag{25}$$

(iii) For triple ionization $\xi^{\mathrm{f}}_{\mathrm{A},q,m}$ depends on the presence of 4d electrons in A^{q+}

$$\xi^{\mathrm{f}}_{\mathrm{A},q,3} = \begin{cases} \xi_{\mathrm{o}} + \xi_{\mathrm{s1}} & \text{for species without 4d electrons} \\ \xi_{\mathrm{o}} + \xi_{\mathrm{s}} & \text{for species with 4d electrons.} \end{cases} \tag{26}$$

Rule (iii) follows from experimental data for isoelectronic sequences of S–Kr and Ag–Bi but we believe that atoms and ions from Y–Pd isoelectronic sequences follow the lower line of expression (26), because a significant change in the number of $\xi^{\mathrm{f}}_{\mathrm{A},q,m}$ is due to the change in status of *M* shell. With the appearance of 4d electrons, the *M* shell becomes the inner one instead of the 'sub-outermost' one, and according to rules (24)–(26) inner shells (the shells below 'sub-outermost') do not contribute to $\xi^{\mathrm{f}}_{\mathrm{A},q,m}$ (for $m \leqslant 4$).

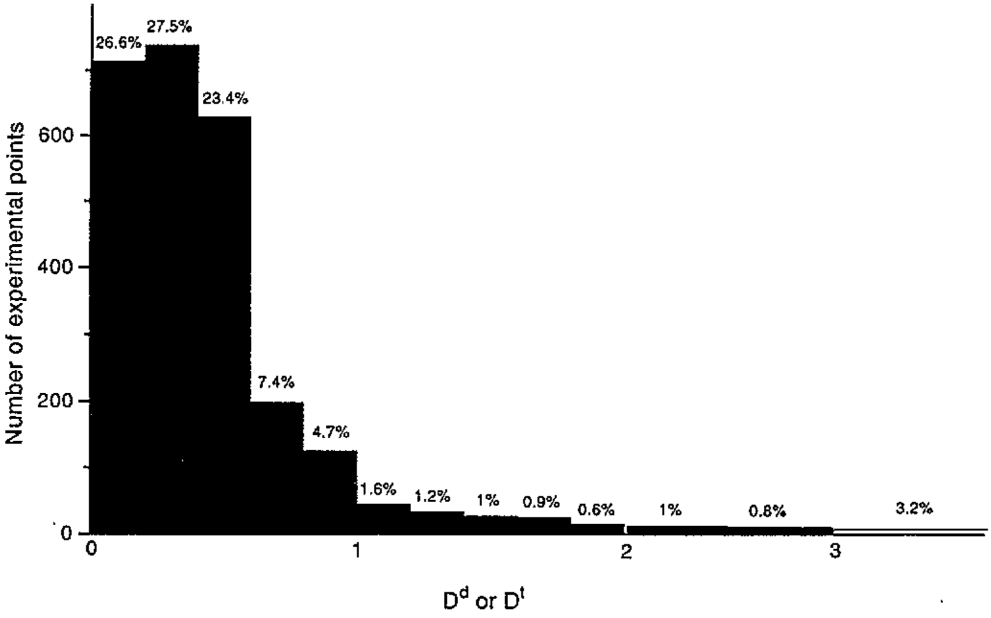

Figure 4. Total distribution of deviations D^{d} and D^{t} for all experimental points presented in figures 1 and 3.

Values of $\xi^{f}_{A,q,m}$ calculated for the majority of atoms are presented in table 3. These values are given in brackets after the notations of shells and subshells participating in the multiple ionization (1) for each value of m. No sign before the notation means that the value $\xi^{f}_{A,q,m}$, calculated according to the rules (24)–(27), provides acceptable scaling of experimental data (figure 3). The plus sign before the notation marks our prediction based on the rules (24)–(27). Experimental data for these atoms are not available as yet. The minus sign marks the shell which provide the best fit to experimental data but contradict our rules. Notation O_l is used for the n_l shell, when it is necessary to distinguish the n_l shell among two n shells coupled in the O shell. Notation S_2 is used for two nl subshells of the S shell, namely, for l_1 and $(l_1 - 1)$ subshells.

In addition to the data related to all atoms from Na to Rn, table 3 contains the data related to ions studied experimentally: Ar^{+}–Ar^{6+}, Rb^{+}, Cs^{+}, Ba^{+}, Ba^{2+}, La^{+}, La^{2+}, Bi^{2+} and Bi^{3+}. One can see that in most examples multiple ionizations of ions are due to transitions in the same subshells as for the atoms of their isoelectronic sequences, i.e. the value $\xi^{f}_{A,q,m}$ depends on the electron configuration, but does not depend on the ion charge. Double ionization of Ar^{5+} and Ar^{6+} and triple ionization of La^{2+} show contributions of more subshells than multiple ionization of an atom from the corresponding isoelectronic sequences, while no example is found where multiple ionization of ions was caused by fewer subshells than those of atoms of the corresponding isoelectronic sequence. This observation may be formulated as the fourth rule: for each value of m the subshells participating in multiple ionization do not change with the increase of q along the isoelectronic sequence, until at some value of q the next subshell starts to participate in m-fold ionization. At present there is not enough data to infer these values for various sequences.

Fivefold ionization was studied only for atoms (namely, the atoms of Ar, Fe, Cu, Kr and Xe). For atoms with no 4d electrons the best accuracy of formula (21) is obtained when $\xi^{f}_{A,q,m}$ is taken equal to the total number of electrons in S and O shells (i.e., equal

Table 3. Electron shells and subshells participating in several-step multiple ionization (columns 6–9) and the numbers $\xi^{f}_{A,q,m}$. Complete n shells with $n = 1, 2, 3, 4$, are denoted by their spectroscopic symbols K, L, M, N. In columns 6–9 the outermost and sub-outermost of the n shells are mentioned by letters O and S. The subscript 1 after the name of the n shell denotes one nl subshell of this n shell, namely the non-empty nl subshell with the largest orbital quantum number. The total number of electrons in the subshells participating in several-step ionization $\xi^{f}_{A,q,m}$ is given in parentheses. Presented results are based on the analysis of experimental data referred in table 2.

Atomic number	A^{q+}	Electron configuration			Electron shells and subshells participating in several-step multiple ionization for various values of m			
		Inner shells	S shell	O shell	$m = 2$	$m = 3$	$m = 4$	$m = 5$
11	Na	K	L	3s	$S_1O(7)$	$+S_1O(7)$	$+SO(9)$	$+SO(9)$
12	Mg	K	L	$3s^2$	$S_1O(8)$	$-KSO(12)$	$-KSO(12)$	$+SO(10)$
13	Al	K	L	$3s^2 3p$	$+S_1O(9)$	$+S_1O(9)$	$+SO(11)$	$+SO(11)$
14	Si	K	L	$3s^2 3p^2$	$S_1O(10)$	$+S_1O(10)$	$+SO(12)$	$+SO(12)$
15	P	K	L	$3s^2 3p^3$	$S_1O(11)$	$+S_1O(11)$	$+SO(13)$	$+SO(13)$
16	S	K	L	$3s^2 3p^4$	$S_1O(12)$	$S_1O(12)$	$-KSO(16)$	$+SO(14)$
17	Cl	K	L	$3s^2 3p^5$	$S_1O(13)$	$+S_1O(13)$	$+SO(15)$	$+SO(15)$
18	Ar	K	L	$3s^2 3p^6$	$+S_1O(14)$	$S_1O(14)$	$SO(16)$	$SO(16)$
18	Ar^{+}	K	L	$3s^2 3p^5$	$+S_1O(13)$	$S_1O(13)$	$+SO(15)$	$+SO(15)$
18	Ar^{2+}	K	L	$3s^2 3p^4$	$S_1O(12)$	$S_1O(12)$	$+SO(14)$	$+SO(14)$
18	Ar^{3+}	K	L	$3s^2 3p^3$	$S_1O(11)$	$+S_1O(11)$	$+SO(13)$	$+SO(13)$
18	Ar^{4+}	K	L	$3s^2 3p^2$	$S_1O(10)$	$+S_1O(10)$	$+SO(12)$	$+SO(12)$
18	Ar^{5+}	K	L	$3s^2 3p$	$-SO(11)$	$+S_1O(9)$	$+SO(11)$	$+SO(11)$
18	Ar^{6+}	K	L	$3s^2$	$-KSO(12)$	$+S_1O(18)$	$+SO(10)$	$+SO(10)$
19	K	K	L	$3s^2 3p^6 4s$	$+S_1O(15)$	$+S_1O(15)$	$+SO(17)$	$+SO(17)$
20	Ca	K	L	$3s^2 3p^6 4s^2$	$S_1O(16)$	$S_1O(16)$	$+SO(18)$	$+SO(18)$
21	Sc	KL	$3s^2 3p^6 3d^1$	$4s^2$	$+S_1O(3)$	$+S_1O(3)$	$+SO(11)$	$+SO(11)$
22	Ti	KL	$3s^2 3p^6 3d^2$	$4s^2$	$+S_1O(4)$	$+S_1O(4)$	$+SO(12)$	$+SO(12)$
23	V	KL	$3s^2 3p^6 3d^3$	$4s^2$	$+S_1O(5)$	$+S_1O(5)$	$+SO(13)$	$+SO(13)$
24	Cr	KL	$3s^2 3p^6 3d^4$	$4s^2$	$+S_1O(6)$	$+S_1O(6)$	$+SO(14)$	$+SO(14)$
25	Mn	KL	$3s^2 3p^6 3d^5$	$4s^2$	$+S_1O(7)$	$+S_1O(7)$	$+SO(15)$	$+SO(15)$
26	Fe	KL	$3s^2 3p^6 3d^6$	$4s^2$	$S_1O(8)$	$+S_1O(8)$	$SO(16)$	$SO(16)$
27	Co	KL	$3s^2 3p^6 3d^7$	$4s^2$	$+S_1O(9)$	$+S_1O(9)$	$+SO(17)$	$+SO(17)$
28	Ni	KL	$3s^2 3p^6 3d^8$	$4s^2$	$+S_1O(10)$	$+S_1O(10)$	$+SO(18)$	$+SO(18)$
29	Cu	KL	M	4s	$S_1O(11)$	$S_1O(11)$	$SO(19)$	$SO(19)$
30	Zn	KL	M	$4s^2$	$+S_1O(12)$	$+S_1O(12)$	$+SO(20)$	$+SO(20)$
31	Ga	KL	M	$4s^2 4p$	$S_1O(13)$	$S_1O(13)$	$+SO(21)$	$+SO(21)$
32	Ge	KL	M	$4s^2 4p^2$	$S_1O(14)$	$S_1O(14)$	$+SO(22)$	$+SO(22)$
33	As	KL	M	$4s^2 4p^3$	$S_1O(15)$	$S_1O(15)$	$+SO(23)$	$+SO(23)$
34	Se	KL	M	$4s^2 4p^4$	$S_1O(16)$	$S_1O(16)$	$+SO(24)$	$+SO(24)$
35	Br	KL	M	$4s^2 4p^5$	$S_1O(17)$	$S_1O(17)$	$+SO(25)$	$+SO(25)$
36	Kr	KL	M	$4s^2 4p^6$	$S_1O(18)$	$S_1O(18)$	$SO(26)$	$SO(26)$
37	Rb	KL	M	$4s^2 4p^6 5s$	$+S_1O(19)$	$+S_1O(19)$	$+SO(27)$	$+SO(27)$
37	Rb^{+}	KL	M	$4s^2 4p^6$	$S_1O(18)$	$S_1O(18)$	$SO(26)$	$+SO(26)$
38	Sr	KL	M	$4s^2 4p^6 5s^2$	$+S_1O(20)$	$+S_1O(20)$	$+SO(28)$	$+SO(28)$
39	Y	KLM	$4s^2 4p^6 4d$	$5s^2$	$+S_1O(3)$	$+SO(11)$	$+SO(11)$	$+M_1SO(21)$
40	Zr	KLM	$4s^2 4p^6 4d^2$	$5s^2$	$+S_1O(4)$	$+SO(12)$	$+SO(12)$	$+M_1SO(22)$
41	Nb	KLM	$4s^2 4p^6 4d^3$	$5s^2$	$+S_1O(5)$	$+SO(13)$	$+SO(13)$	$+M_1SO(23)$
42	Mo	KLM	$4s^2 4p^6 4d^4$	$5s^2$	$+S_1O(6)$	$+SO(14)$	$+SO(14)$	$+M_1SO(24)$
43	Tc	KLM	$4s^2 4p^6 4d^5$	$5s^2$	$+S_1O(7)$	$+SO(15)$	$+SO(15)$	$+M_1SO(25)$
44	Ru	KLM	$4s^2 4p^6 4d^7$	5s	$+S_1O(8)$	$+SO(16)$	$+SO(16)$	$+M_1SO(26)$
45	Rh	KLM	$4s^2 4p^6 4d^8$	5s	$+S_1O(9)$	$+SO(17)$	$+SO(17)$	$+M_1SO(27)$
46	Pd	KL	M	$4s^2 4p^6 4d^{10}$	$+S_1O(28)$	$+SO(36)$	$+SO(36)$	$+L_1SO(42)$
47	Ag	KLM	$4s^2 4p^6 4d^{10}$	5s	$S_1O(11)$	$SO(19)$	$+SO(19)$	$+M_1SO(29)$
48	Cd	KLM	$4s^2 4p^6 4d^{10}$	$5s^2$	$+S_1O(12)$	$+SO(20)$	$+SO(20)$	$+M_1SO(30)$

Table 3. (continued)

Atomic number	A^{q+}	Electron configuration			Electron shells and subshells participating in several-step multiple ionization for various values of *m*			
		Inner shells	S shell	O shell	$m = 2$	$m = 3$	$m = 4$	$m = 5$
49	In	KLM	$4s^24p^64d^{10}$	$5s^25p$	$S_1O(13)$	$SO(21)$	$+SO(21)$	$+M_1SO(31)$
50	Sn	KLM	$4s^24p^64d^{10}$	$5s^25p^2$	$S_1O(14)$	$SO(22)$	$+SO(22)$	$+M_1SO(32)$
51	Sb	KLM	$4s^24p^64d^{10}$	$5s^25p^3$	$S_1O(15)$	$SO(23)$	$+SO(23)$	$+M_1SO(33)$
52	Te	KLM	$4s^24p^64d^{10}$	$5s^25p^4$	$S_1O(16)$	$SO(24)$	$+SO(24)$	$+M_1SO(34)$
53	I	KLM	$4s^24p^64d^{10}$	$5s^25p^5$	$S_1O(17)$	$SO(25)$	$+SO(25)$	$+M_1SO(35)$
54	Xe	KLM	$4s^24p^64d^{10}$	$5s^25p^6$	$S_1O(18)$	$SO(26)$	$SO(26)$	$M_1SO(36)$
55	Cs	KLM	$4s^24p^64d^{10}$	$5s^25p^66s$	$+S_1O(19)$	$+SO(27)$	$+SO(27)$	$+M_1SO(37)$
55	Cs^+	KLM	$4s^24p^64d^{10}$	$5s^25p^6$	$S_1O(18)$	$SO(26)$	$SO(26)$	$+M_1SO(36)$
56	Ba	KLM	$4s^24p^64d^{10}$	$5s^25p^66s^2$	$S_1O(20)$	$SO(28)$	$SO(28)$	$+M_1SO(38)$
56	Ba^+	KLM	$4s^24p^64d^{10}$	$5s^25p^66s$	$S_1O(19)$	$+SO(27)$	$+SO(27)$	$+M_1SO(37)$
56	Ba^{2+}	KLM	$4s^24p^64d^{10}$	$5s^25p^6$	$S_1O(18)$	$+SO(26)$	$+SO(26)$	$+M_1SO(36)$
57	La	KLM	$4s^24p^64d^{10}$	$5s^25p^65d^16s^2$	$+S_1O(21)$	$+SO(29)$	$+SO(29)$	$+M_1SO(39)$
57	La^+	KLM	$4s^24p^64d^{10}$	$5s^25p^66s^2$	$S_1O(20)$	$+SO(28)$	$+SO(28)$	$+M_1SO(38)$
57	La^{2+}	KLM	$4s^24p^64d^{10}$	$5s^25p^66s$	$S_1O(19)$	$-MSO(45)$	$+SO(27)$	$+M_1SO(37)$
58	Ce	KLM	$4s^24p^64d^{10}4f^2$	$5s^25p^66s^2$	$+S_1O(12)$	$+SO(30)$	$+SO(30)$	$+M_1SO(40)$
59	Pr	KLM	$4s^24p^64d^{10}4f^3$	$5s^25p^66s^2$	$+S_1O(13)$	$+SO(31)$	$+SO(31)$	$+M_1SO(41)$
60	Nd	KLM	$4s^24p^64d^{10}4f^4$	$5s^25p^66s^2$	$+S_1O(14)$	$+SO(32)$	$+SO(32)$	$+M_1SO(42)$
61	Pm	KLM	$4s^24p^64d^{10}4f^5$	$5s^25p^66s^2$	$+S_1O(15)$	$+SO(33)$	$+SO(33)$	$+M_1SO(43)$
62	Sm	KLM	$4s^24p^64d^{10}4f^6$	$5s^25p^66s^2$	$S_1O(16)$	$-S_2O(26)$	$+SO(34)$	$+M_1SO(44)$
63	Eu	KLM	$4s^24p^64d^{10}4f^7$	$5s^25p^66s^2$	$S_1O(17)$	$-S_2O(27)$	$+SO(35)$	$+M_1SO(45)$
64	Gd	KLM	$4s^24p^64d^{10}4f^7$	$5s^25p^65d^16s^2$	$+S_1O(18)$	$+SO(36)$	$+SO(36)$	$+M_1SO(46)$
65	Tb	KLM	$4s^24p^64d^{10}4f^9$	$5s^25p^66s^2$	$+S_1O(19)$	$+SO(37)$	$+SO(37)$	$+M_1SO(47)$
66	Dy	KLM	$4s^24p^64d^{10}4f^{10}$	$5s^25p^66s^2$	$+S_1O(20)$	$+SO(38)$	$+SO(38)$	$+M_1SO(48)$
67	Ho	KLM	$4s^24p^64d^{10}4f^{11}$	$5s^25p^66s^2$	$+S_1O(21)$	$+SO(39)$	$+SO(39)$	$+M_1SO(49)$
68	Er	KLM	$4s^24p^64d^{10}4f^{12}$	$5s^25p^66s^2$	$+S_1O(22)$	$+SO(40)$	$+SO(40)$	$+M_1SO(50)$
69	Tm	KLM	$4s^24p^64d^{10}4f^{13}$	$5s^24p^66s^2$	$-S_1O_1(15)$	$-S_1O(23)$	$+SO(41)$	$+M_1SO(51)$
70	Yb	KLM	N	$5s^25p^66s^2$	$-S_1O_1(16)$	$-S_1O(24)$	$+SO(42)$	$+M_1SO(52)$
71	Lu	KLMN	$5s^25p^65d^1$	$6s^2$	$+S_1O(3)$	$+SO(11)$	$+SO(11)$	$+N_1SO(25)$
72	Hf	KLMN	$5s^25p^65d^2$	$6s^2$	$+S_1O(4)$	$+SO(12)$	$+SO(12)$	$+N_1SO(26)$
73	Ta	KLMN	$5s^25p^65d^3$	$6s^2$	$+S_1O(5)$	$+SO(13)$	$+SO(13)$	$+N_1SO(27)$
74	W	KLMN	$5s^25p^65d^4$	$6s^2$	$+S_1O(6)$	$+SO(14)$	$+SO(14)$	$+N_1SO(28)$
75	Re	KLMN	$5s^25p^65d^5$	$6s^2$	$+S_1O(7)$	$+SO(15)$	$+SO(15)$	$+N_1SO(29)$
76	Os	KLMN	$5s^25p^65d^6$	$6s^2$	$+S_1O(8)$	$+SO(16)$	$+SO(16)$	$+N_1SO(30)$
77	Ir	KLMN	$5s^25p^65d^7$	$6s^2$	$+S_1O(9)$	$+SO(17)$	$+SO(17)$	$+N_1SO(31)$
78	Pt	KLMN	$5s^25p^65d^9$	$6s$	$+S_1O(10)$	$+SO(18)$	$+SO(18)$	$+N_1SO(32)$
79	Au	KLMN	$5s^25p^65d^{10}$	$6s$	$+S_1O(11)$	$+SO(19)$	$+SO(19)$	$+N_1SO(33)$
80	Hg	KLMN	$5s^25p^65d^{10}$	$6s^2$	$+S_1O(12)$	$+SO(20)$	$+SO(20$	$+N_1SO(34)$
81	Tl	KLMN	$5s^25p^65d^{10}$	$6s^26p$	$+S_1O(13)$	$+SO(21)$	$+SO(21)$	$+N_1SO(35)$
82	Pb	KLMN	$5s^25p^65d^{10}$	$6s^26p^2$	$S_1O(14)$	$SO(22)$	$+SO(22)$	$+N_1SO(36)$
83	Bi	KLMN	$5s^25p^65d^{10}$	$6s^26p^3$	$S_1O(15)$	$SO(23)$	$+SO(23)$	$+N_1SO(37)$
83	Bi^{2+}	KLMN	$5s^25p^65d^{10}$	$6s^26p$	$S_1O(13)$	$+SO(21)$	$+SO(21)$	$+N_1SO(35)$
83	Bi^{3+}	KLMN	$5s^25p^65d^{10}$	$6s^2$	$S_1O(12)$	$+SO(20)$	$+SO(20)$	$+N_1SO(34)$
84	Po	KLMN	$5s^25p^65d^{10}$	$6s^26p^4$	$+S_1O(16)$	$+SO(24)$	$+SO(24)$	$+N_1SO(38)$
85	At	KLMN	$5s^25p^65d^{10}$	$6s^26p^5$	$+S_1O(17)$	$+SO(25)$	$+SO(25)$	$+N_1SO(39)$
86	Rn	KLMN	$5s^25p^65d^{10}$	$6s^26p^6$	$+S_1O(18)$	$+SO(26)$	$+SO(26)$	$+N_1SO(40)$

values of $\xi^f_{A,q,m}$ for $m = 4$ and $m = 5$). To explain fivefold ionization of xenon one has to assume that the last subshell of the inner shell (namely, the 3d subshell) also participates in several-step processes. We believe that the l_1 subshell of the last inner shell participates in several-step fivefold ionization of all species with 4d electrons:

$$\xi^{\mathrm{f}}_{\mathrm{A},q,5} = \begin{cases} \xi_{\mathrm{o}} + \xi_{\mathrm{s}} & \text{for species without 4d electrons} \\ \xi_{\mathrm{o}} + \xi_{\mathrm{s}} + \xi_{I1} & \text{for species with 4d electrons.} \end{cases} \tag{27}$$

Here, I denotes the n shell with $n = n_{\mathrm{s}} - 1$; number ξ_{I1} is the number of electrons in the last non-empty subshell of this shell and n_{s} is the principal quantum number of the S shell.

Also a sixth rule may be established: for any atom or ion the increase of m is never followed by a decrease of $\xi^{\mathrm{f}}_{\mathrm{A},q,m}$; on the contrary, for larger values of m more subshells contribute to $\xi^{\mathrm{f}}_{\mathrm{A},q,m}$. Six-, seven- and eightfold ionization was studied only for atomic krypton [13], and this study gives a good example of the sixth rule: the shells contributing to m-fold ionization for increasing values of m are: $\mathrm{S_1O}$ for $m = 2$ and 3, SO for $m = 4$ and 5, $\mathrm{I_1SO}$ for $m = 6$, ISO for $m = 7$ and 8.

The scaling (21) demonstrated in figure 3 is an argument to expect scaling for all species which have more than ten electrons (i.e. having electrons above complete K and L shells). Then the electron-impact multiple ionization cross sections of these species may be presented as

$$\sigma_{\mathrm{A},q,m}(x) = S^{\mathrm{t}}_{\mathrm{A},q,m}\tilde{\sigma}^{\mathrm{t}}_{\mathrm{u}}(x) \qquad x > x^{\mathrm{t}}_{\mathrm{A},q,m}. \tag{28}$$

Using formulae (17) and (22), expression (28) may be presented in the more explicit form:

$$\sigma_{\mathrm{A},q,m}(x) = 1.6\frac{\pi a_0^2}{17^{m-1}}\left(\frac{I_{\mathrm{H}}}{I_{\mathrm{A},q,m}}\right)^2 \zeta^{\mathrm{t}}_{\mathrm{A},q,m}\frac{\ln x}{x^{0.9}}\left(1 - 2\mathrm{e}^{-0.7x}\right) \qquad x > x^{\mathrm{t}}_{\mathrm{A},q,m}. \tag{29}$$

4. Cross sections for the entire range $x \geqslant 1$

For applications, it is desirable to have a method to determine multiple ionization cross sections for arbitrary energy of the projectile electron. Here we propose a method based on the regularities in threshold values $x^{\mathrm{i}}_{\mathrm{A},q,m}$ and $x^{\mathrm{t}}_{\mathrm{A},q,m}$. It can be seen in tables 1 and 2 that species A^{q+} with no M shell usually have high thresholds $x^{\mathrm{i}}_{\mathrm{A},q,m}$ (all species studied except for C^+ have values $x^{\mathrm{i}}_{\mathrm{A},q,m}$ larger than maximal energy in the range of measurements) while species with M shells usually have $x^{\mathrm{t}}_{\mathrm{A},q,m}$ not far from unity.

Therefore, for an arbitrary energy of a projectile electron, the cross section can be estimated as follows. If species A^{q+} has no M shell, $x^{\mathrm{i}}_{\mathrm{A},q,m}$ can be assumed infinite, and expression (10) can be used for any value of x. If species A^{q+} has an M shell, $x^{\mathrm{t}}_{\mathrm{A},q,m}$ can be assumed to be unity and expression (29) can be used for any value of x. The results obtained for atomic copper and krypton using this method are shown in figures 5 and 6. The cross sections (29) are presented by full curves (thick for $x > x^{\mathrm{t}}_{\mathrm{A},q,m}$ and thin for $x < x^{\mathrm{t}}_{\mathrm{A},q,m}$). Qualitatively, the expression (29) fits well both sequences of the experimental cross sections in the six orders of magnitude range of values (from 10^{-23} to 10^{-17} cm^2). Quantitatively, the deviations of full curves from the experimental data are within a factor of four for $m = 2, 3, 4, 5$. For $m > 5$ the deviations are larger at $x \approx 1$, but it may be due to inaccuracy of equality (2).

Dotted curves present one-step cross sections (10). It is seen that when $x^{\mathrm{i}}_{\mathrm{A},q,m}$ is large (as for double ionization of copper) formula (10) in its validity range is much more accurate than the extrapolation of formula (29) into this range. Therefore, if for any species the

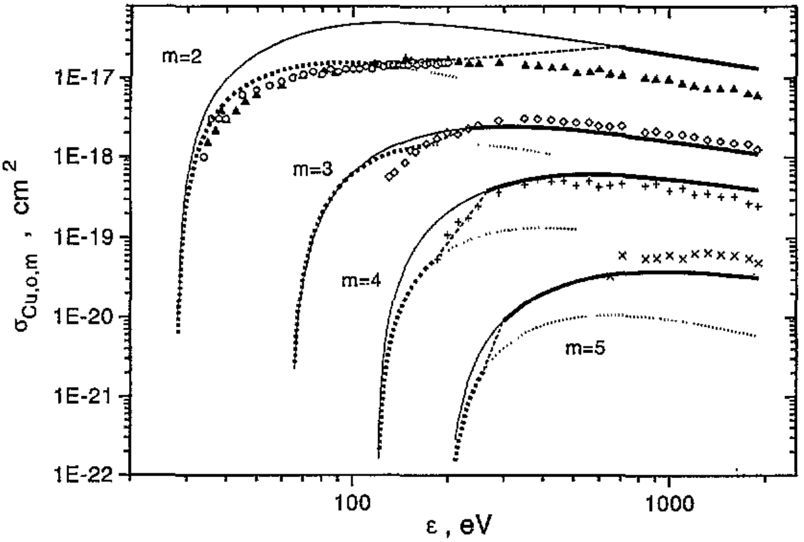

Figure 5. Multiple ionization cross sections of copper atoms ($m = 2, 3, 4, 5$). Experiment: open circles, Freund *et al* [5], all other symbols, Bolorizadeh *et al* [2]. Our calculations using formula (10) for one-step multiple ionization are presented by thick dotted curves in the validity range $x < x^{\mathrm{i}}_{\mathrm{A},q,m}$ and continued as thin dotted curves into the range $x > x^{\mathrm{i}}_{\mathrm{A},q,m}$. Total multiple ionization cross sections (29) are shown by full curves (thick in the validity range of (29) and continued as thin when calculated for $x < x^{\mathrm{t}}_{\mathrm{A},q,m}$). Linear interpolation between $x^{\mathrm{i}}_{\mathrm{A},q,m}$ and $x^{\mathrm{t}}_{\mathrm{A},q,m}$ is shown by a broken segment.

values $x^{\mathrm{i}}_{\mathrm{A},q,m}$ and $x^{\mathrm{t}}_{\mathrm{A},q,m}$ are known (from analysis of atomic structure or from analysis of the values known for other atoms and ions) one may use for this species expressions (10) and (29) in their ranges of validity, while in the intermediate range $x^{\mathrm{i}}_{\mathrm{A},q,m} < x < x^{\mathrm{t}}_{\mathrm{A},q,m}$ the cross sections may be calculated by linear interpolation between $\sigma_1 = \sigma_{\mathrm{A},q,m}(x^{\mathrm{i}}_{\mathrm{A},q,m})$ and $\sigma_2 = \sigma_{\mathrm{A},q,m}(x^{\mathrm{t}}_{\mathrm{A},q,m})$:

$$\sigma_{\mathrm{A},q,m}(x) = \sigma_1 + \frac{x - x^{\mathrm{i}}_{\mathrm{A},q,m}}{x^{\mathrm{t}}_{\mathrm{A},q,m} - x^{\mathrm{i}}_{\mathrm{A},q,m}}(\sigma_2 - \sigma_1) \qquad x^{\mathrm{i}}_{\mathrm{A},q,m} < x < x^{\mathrm{t}}_{\mathrm{A},q,m}. \tag{30}$$

An example of this linear interpolation is shown in figure 5 by broken curves. For $m = 2$, 3, 4, the values $x^{\mathrm{i}}_{\mathrm{A},q,m}$ and $x^{\mathrm{t}}_{\mathrm{A},q,m}$ are inferred from experimental data. It is seen that when these values are known it is more accurate to calculate the cross sections by the interpolation (30) than to use expression (28) in the entire range $x \geqslant 1$. For $m = 5$, values $x^{\mathrm{i}}_{\mathrm{A},q,m}$ and $x^{\mathrm{t}}_{\mathrm{A},q,m}$ cannot be obtained from available data, and an interpolation segment is drawn rather arbitrarily.

5. Electron-impact multiple ionization of negative ions

Scaling law (7) was inferred from experimental data for atoms and positive atomic ions. Figure 7 demonstrates that the electron-impact cross section for double ionization of negative in H$^-$ is also in reasonable agreement with this scaling law. On the basis of similarity of negative ions and atoms from the view point of multiple ionization, we expect that expressions (10) and (29) will be reasonably accurate in the prediction of electron-impact multiple ionization cross sections for all negative atomic ions. Expression (10) is

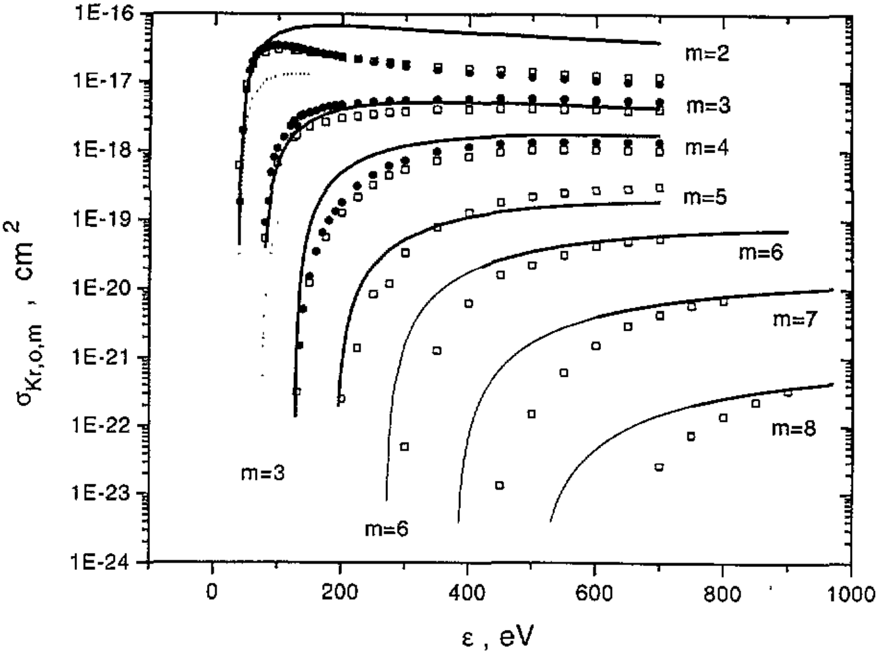

Figure 6. Multiple ionization cross sections of krypton atoms ($m = 2, 3, \ldots, 8$). Experiment: open squares, Lebius *et al* [13]; full symbols, Krishnakumar and Srivastava [12]. Our calculations using formulae (10) for one-step multiple ionization cross sections and (29) for total multiple ionization cross sections are presented by dotted and full curves respectively. In the ranges $x > x^{t}_{A,q,m}$ full curves are made wider. For $m > 3$ the one-step ionization cross sections (10) are not shown because the validity thresholds $x^{i}_{A,q,m}$ are close to unity.

recommended for ions H$^-$, He$^-$, Li$^-$, B$^-$, C$^-$, O$^-$ and F$^-$. Ions Be$^-$, N$^-$, Ne$^-$, Mg$^-$ do not exist [36]. For ions Na$^-$, Al$^-$ and heavier ones we recommend expression (29). In both the expressions the attached electron has to be treated as one of the electrons of the outermost n shell.

6. Conclusions

Experimentally determined electron-impact multiple ionization cross sections [2–30, 38] satisfy a scaling relation (7) in the energy range $1 < x < x^{i}_{A,q,m}$ and a scaling relation (21) in the energy range $x > x^{t}_{A,q,m}$. For the majority of species the accuracy of these relations is within a factor of two.

Based on these scaling relations we propose the formula (10) for calculating the cross section in the range $1 < x < x^{i}_{A,q,m}$ and the formula (29) for calculating the cross sections in the range $x > x^{t}_{A,q,m}$.

To estimate the multiple ionization cross sections for an arbitrary energy of projectile electron ($x \geqslant 1$) one may use formula (10) for species with ten or less electrons (i.e. with one or two electron shells), and formula (29) for species with eleven or more electrons (i.e. with three or more electron shells).

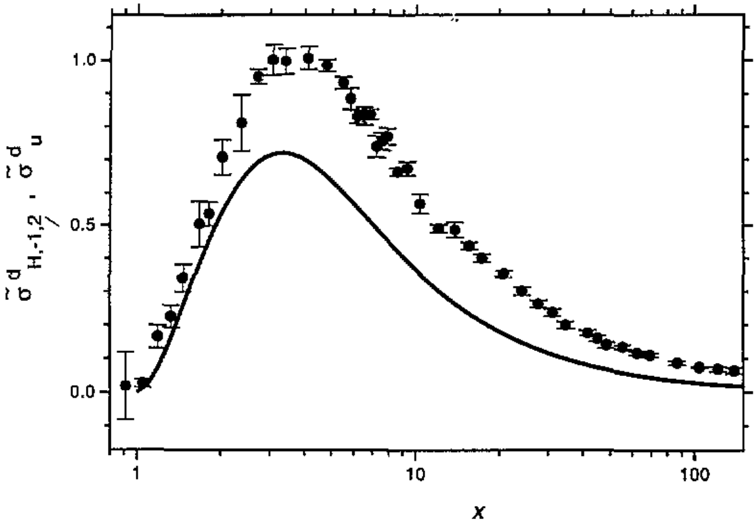

Figure 7. Universal cross section (8), full curve compared with scaled experimental cross section for double ionization of negative ion H^- by electron impact. Experimental data from the paper by Yu *et al* [38].

Acknowledgments

It is a pleasure to acknowledge fruitful discussions with Sergei I Anisimov and Leonid A Vainshtein. We are grateful to NIFS (Japan) and H Tawara for giving us the opportunity to use the NIFS atomic database. This work was supported by the Israeli Academy of Science, Ministry of Science and Arts, and the Ministry of Absorption.

References

[1] Müller A 1986 *Phys. Lett.* **113A** 415–9
[2] Bolorizadeh M A, Patton C J, Shah M B and Gilbody H B 1994 *J. Phys. B: At. Mol. Opt. Phys.* **27** 175–83
[3] Chatterjee S N and Roy B N 1984 *J. Phys. B: At. Mol. Phys.* **17** 2527–34
[4] Dettman J M and Karstensen F 1982 *J. Phys. B: At. Mol. Phys.* **15** 287–300
[5] Freund R S, Wetzel R C, Shul R J and Hayes T R 1990 *Phys. Rev.* A **41** 3575–95
[6] Hayes T R, Wetzel R C and Freund R S 1987 *Phys. Rev.* A **35** 578–84
[7] Herting D R, Feeney R K, Hughes D W and Sayle W E II 1982 *J. Appl. Phys.* **53** 5427–34
[8] Hughes D W and Feeney R K 1981 *Phys. Rev.* A **23** 2241–9
[9] Gaudin A and Hagemann R 1967 *J. Chim. Phys.* **64** 1209–21
[10] Hirayama T, Oda K, Morikawa Y, Ono T, Ikezaki Y, Takayanagi T, Wakiya K and Suzuki H 1986 *J. Phys. Soc. Japan* **55** 1411–4
[11] Jalin R, Hagemann R and Botter R 1973 *J. Chem. Phys.* **59** 952–9
[12] Krishnakumar E and Srivastava S K 1988 *J. Phys. B: At. Mol. Opt. Phys.* **21** 1055–82
[13] Lebius H, Binder J, Koslowski H R, Wiesemann K and Huber B A 1989 *J. Phys. B: At. Mol. Opt. Phys.* **22** 83–97
[14] McCallion P, Shah M B and Gilbody H B 1992 *J. Phys. B: At. Mol. Opt. Phys.* **25** 1051–60
[15] McCallion P, Shah M B and Gilbody H B 1992 *J. Phys. B: At. Mol. Opt. Phys.* **25** 1061–71
[16] Müller A and Frodl R 1980 *Phys. Rev. Lett.* **44** 29–32
[17] Müller A, Tinschert K, Achenbach C, Becker R and Salzborn E 1985 *J. Phys. B: At. Mol. Phys.* **18** 3011–6
[18] Müller A, Tinschert K, Achenbach C, Salzborn E, Becker R and Pindzola M S 1985 *Phys. Rev. Lett.* **54** 414–7

[19] Müller A, Tinschert K, Hofmann G, Salzborn E, Dunn G H, Younger S M and Pindzola M S 1989 *Phys. Rev.* A **40** 3584–98

[20] Nagy P, Skutlartz A and Schmidt V 1980 *J. Phys. B: At. Mol. Phys.* **13** 1249–67

[21] Peart B and Dolder K T 1969 *J. Phys. B: At. Mol. Phys.* **2** 1169–75

[22] Peart B, Green S J T and Thomason J W G 1993 *J. Phys. B: At. Mol. Opt. Phys.* **26** 149–55

[23] Shah M B, Elliott D S, McCallion P and Gilbody H B 1988 *J. Phys. B: At. Mol. Opt. Phys.* **21** 2751–61

[24] Shimon L L, Volovich P N and Chiriban M M 1989 *Sov. Phys.–Tech. Phys.* **34** 1264–6

[25] Syage J A 1992 *Phys. Rev.* A **46** 5666–79

[26] Tinschert K, Müller A, Phaneuf R A, Hoffmann G and Salzborn E 1989 *J. Phys. B: At. Mol. Opt. Phys.* **22** 1241–8

[27] Tinschert K, Müller A, Hofmann G, Salzborn E and Younger S M 1991 *Phys. Rev.* A **43** 3522–34

[28] Wetzel R C, Baiocchi F A, Hayes T R and Freund R S 1987 *Phys. Rev.* A **35** 578–84

[29] Zambra M, Belic D, Defrance P and Yu D J 1994 *J. Phys. B: At. Mol. Opt. Phys.* **27** 2383–97

[30] Ziegler D L, Newman J H, Smith K A and Stebbings R F 1982 *Planet Space Sci.* **30** 451–6

[31] Müller A 1991 *Physics of Ion Impact Phenomena* ed D Mathur (Berlin: Springer) pp 13–90

[32] Müller A 1991 *Comment. At. Mol. Phys.* **27** 1–23

[33] Dolder K 1994 *Adv. At. Mol. Opt. Phys.* **32** 69–92

[34] Wannier G H 1955 *Phys. Rev.* **100** 1180

[35] Gryzinski M 1965 *Phys. Rev.* **138** A305–35

[36] Radzig A A and Smirnov B M 1986 *Parameters of Atoms and Atomic Ions* (Moscow: Energoatomizdat) (in Russian)

[37] Cowan R D 1981 *The Theory of Atomic Structure and Spectra* (Berkeley, CA: University of California Press)

[38] Yu D J, Rachafi S, Jureta J and Defrance P 1992 *J. Phys. B: At. Mol. Opt. Phys.* **25** 4593–600